Cu(I) and Ag(I) complexes of 7-azaindolyl and 2,2′-dipyridylamino substituted 1,3,5-triazine and benzene: the central core impact on structure, solution dynamics and fluorescence of the complexes†

Elizabeth Wong, John Li, Corey Seward and Suning Wang*

Received 19th August 2008, Accepted 14th November 2008
First published as an Advance Article on the web 27th January 2009
DOI: 10.1039/b814393e

The interactions of Cu(I) and Ag(I) ions with four star-shaped ligands, 2,4,6-tris(*N*-7-azaindolyl)-1,3,5-triazine (tat), 1,3,5-tris(*N*-7-azaindolyl)benzene (tab), 2,4,6-tris(2,2′-dipyridylamino)-1,3,5-triazine (tdat) and 1,3,5-tris(2,2′-dipyridylamino)benzene (tdab) have been investigated by X-ray diffraction, NMR and fluorescent spectroscopic analyses. Eight new complexes $[Cu(PPh_3)(tat)][BF_4]$ (**1**), $[Cu(PPh_3)(tab)][BF_4]$ (**2**), $[Cu(PPh_3)(tdab)][BF_4]$ (**3**), $\{[Cu(PPh_3)_2]_2(tdat)]\}[BF_4]_2$ (**4**), $(AgNO_3)_{1.5}(tab)$ (**5**), $(AgNO_3)_2(tat)$ (**6**), $(AgNO_3)_4(tdab)$ (**7**), and $(AgNO_3)_3(tdat)(H_2O)_2$ (**8**) have been isolated from the reactions of $[Cu(PPh_3)_2(CH_3CN)_2][BF_4]$ and $AgNO_3$ with the corresponding ligands. The structures of compounds **1–7** have been established by single-crystal X-ray diffraction analyses, which show that the central core in the chelate ligand results in distinct structures for both Cu(I) and Ag(I) complexes. All Cu(I) complexes are discrete molecules while all Ag(I) complexes are polymeric with helical, sandwich, or chair-like structures. A variable temperature ^1H NMR study established that the Cu(I) complexes display dynamic exchange in solution. Fluorescent titration experiments showed that the four ligands have distinct responses toward Cu(I) and Ag(I) ions, which may be correlated to the distinct structures of the complexes and the electronic property differences of the ligands.

Introduction

The study of metal–ligand interactions is the core of modern inorganic chemistry. Understanding metal–ligand interactions allows us to design and synthesize new complexes and materials that have the desired properties for targeted applications.[1] Our group has been particularly interested in the interactions of metal ions with luminescent ligands because of their relevance in the development of phosphorescent materials for optoelectronic devices,[2] photochemically active materials[3] and sensor materials.[4] Among the ligand systems that have been examined by our group, 7-azaindolyl and 2,2′-dipyridylamino derivative ligands with a central triazine or benzene core and a 3-fold symmetry such as 2,4,6-tris(*N*-7-azaindolyl)-1,3,5-triazine (tat), 1,3,5-tris(*N*-7-azaindolyl)benzene (tab), 2,4,6-tris(2,2′-dipyridylamino)-1,3,5-triazine (tdat) and 1,3,5-tris(2,2′-dipyridylamino)benzene (tdab) (shown in Chart 1), are the most attractive because of the presence of multiple binding sites and the highly emissive nature of the ligands.[5] Previously, we have shown that the tdab and tdat ligands can bind readily to Zn(II), Pd(II) and Pt(II) *via* either the 2,2′-dipyridylamino chelate or N,C,N-cyclometallation to form mononuclear, dinuclear or trinuclear coordination or organometallic compounds that have distinct structural features and luminescent properties.[4d,6] We have also shown that the tab ligand can readily form phosphorescent N,C,N-cyclometallated complexes with either a Pd(II) or Pt(II) center.[7] Our current investigation focuses on the interactions of Cu(I) and Ag(I) ions with this group of ligands. Our interests in Cu(I) complexes are motivated by several recent reports of highly efficient organic light-emitting devices based on phosphorescent Cu(I) complexes with N,N-chelate ligands.[8] Ag(I) is in the same family as Cu(I), but has a greater tendency to form polymeric species than Cu(I).[1,9] To compare the difference between these two metal ions toward the 7-azaindolyl and 2,2′-dipyridylamino functionalized ligands, we also examined the interactions of Ag(I) with tat, tab, tdab and tdat ligands. The details are presented herein.

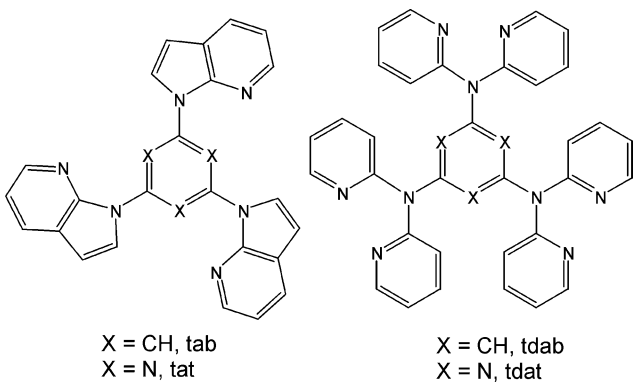

Chart 1

Department of Chemistry, Queen's University, Kingston, Ontario, K7L 3N6, Canada. E-mail: wangs@chem.queensu.ca

† Electronic supplementary information (ESI) available: ^1H NMR, UV-Vis and fluorescence spectra of complexes. CCDC reference numbers 699116–699122. For ESI and crystallographic data in CIF or other electronic format see DOI: 10.1039/b814393e

Experimental

General procedures

All starting reagents and reagent grade solvents were purchased from Aldrich Chemical Company and used without further purification. The starting material $[Cu(CH_3CN)_2(PPh_3)_2][BF_4]$ was prepared from literature procedures,[10] while tat, tab, tdab and tdat ligands were prepared according to the procedures reported previously by our group.[5] The ^1H NMR and ^{13}C NMR spectra were recorded on either Bruker Avance 300 MHz, 400 MHz or 500 MHz spectrometers. Emission and excitation spectra were recorded on a Photon Technologies International QuantaMaster Model C-60 Spectrometer. UV-Vis spectra were recorded on an Ocean Optics UV-Vis spectrophotometer. Elemental analyses were performed by Canadian Microanalytical Service Ltd., Delta, British Columbia, Canada and by the Analytical Laboratory for Environmental Science Research and Training, University of Toronto, Toronto, Ontario, Canada.

Synthesis of $[(CuPPh_3)(tat)][BF_4]$, (1). Under nitrogen, a solution of $[Cu(CH_3CN)_2(PPh_3)][BF_4]$ (0.106 g, 0.140 mmol) in CH_2Cl_2 was added to a solution of tat (0.030 g, 0.070 mmol) in the same solvent. The reaction was carried out in a molar ratio of 1 : 2. The mixture was stirred for 1 min and was then layered with hexanes. The crystals formed with difficulty and the solution required repeated cycles of dissolution and hexanes layering. Crystals of **1** were isolated in 72% yield. Mp >282 °C (decomposition). ^1H NMR (CD_2Cl_2, 500 MHz, 298K, δ, ppm): 8.65 (dd, $J = 5.0$ Hz, $J = 1.6$ Hz, 2H, 7-aza), 8.60 (d, $J = 4.0$ Hz, 2H, 7-aza), 8.55 (dd, $J = 4.8$ Hz, $J = 1.6$ Hz, 1H, 7-aza), 8.23 (d, $J = 4.4$ Hz, 1H, 7-aza), 8.18 (dd, $J = 8.0$ Hz, $J = 1.6$ Hz, 2H, 7-aza), 8.00 (dd, $J = 7.6$ Hz, $J = 1.6$ Hz, 1H, 7-aza), 7.48 (dd, $J = 8.0$ Hz, $J = 5.2$ Hz, 1H, 7-aza), 7.32 (dd, $J = 7.0$ Hz, $J = 4.8$ Hz, 1H, 7-aza), 7.28 (m, 3H, ph), 7.17 (m, 6H, ph), 6.92 (m, 6H, ph), 6.82 (d, $J = 4.4$ Hz, 1H, 7-aza). ^{13}C NMR (CD_2Cl_2, 300 MHz, 298K, δ, ppm): 206.7, 161.5, 149.1, 146.9, 145.7, 145.1, 132.8, 132.6, 132.4, 132.3, 132.0, 130.5, 130.0, 129.2, 129.1, 128.2, 127.2, 125.7, 125.1, 121.2, 120.2, 108.6. Anal. calcd. for $C_{42}H_{30}N_9CuPBF_4$: C, 59.90; H, 3.60; N, 14.97. Found: C, 60.13; H, 3.32; N, 14.94%.

Synthesis of $[(CuPPh_3)(tab)][BF_4]$, (2). Under nitrogen, tab (0.023 g, 0.059 mmol) was mixed with $[Cu(CH_3CN)_2(PPh_3)][BF_4]$ (0.177 g, 0.234 mmol) in CH_2Cl_2 in a molar ratio of 1 : 4. Hexanes were then layered on top. The mixture was stirred for 1 min and the overnight reaction at room temperature yielded colorless, rectangular crystals of compound **2** in 65% yield. Mp >280 °C (decomposition). ^1H NMR (CD_2Cl_2, 300 MHz, 298K, δ, ppm): 8.50 (s, 3H, 7-aza), 8.22 (d, $J = 7.5$ Hz, 3H, 7-aza), 7.72 (s, 3H, benzene), 7.37 (dd, $J = 7.8$ Hz, $J = 4.5$ Hz, 3H, 7-aza), 7.20 (m, 3H, ph), 7.02 (m, 6H, ph), 6.88 (d, $J = 3.6$, 3H, 7-aza), 7.79 (m, 6H, Ph), ^{13}C NMR (CD_2Cl_2, 298K, δ, ppm): 143.6, 133.9, 133.1, 132.9, 131.5, 130.8, 129.6,129.1. Anal. calcd. for $C_{45}H_{32}N_6CuPBF_4{\cdot}CH_2Cl_2$: C, 59.85; H, 3.72; N, 9.10. Found: C, 60.32; H, 3.69; N, 8.81%.

Synthesis of $[(CuPPh_3)(tdab)][BF_4]$, (3). Under nitrogen gas, tdab (0.025 g, 0.043 mmol) and $[Cu(CH_3CN)_2(PPh_3)_2][BF_4]$. (0.097 g, 140 mmol) were combined in a molar ratio of 1 : 1 in CH_2Cl_2. Hexanes and THF were then layered on top. After several days, transparent light yellow crystals of **3** were isolated in 43% yield. Mp >250 °C (decomposition). ^1H NMR (CD_2Cl_2, 400 MHz, 298K, δ, ppm): 8.14 (d, $J = 4.0$ Hz, 6H, py), 7.53 (dd, $J = 8.7$ Hz, $J = 8.0$ Hz, 6H, py), 7.37 (m, 15H, ph), 7.01 (dd, $J = 8.7$ Hz, $J = 4.0$ Hz, py), 6.81 (d, $J = 8.0$ Hz, 6H, py), 6.31 (s, 3H, central phenyl). Anal. calcd. for $C_{54}H_{45}CuN_9PBF_4{\cdot}THF$: C, 64.97; H, 4.24; N, 12.63. Found: C, 63.81; H, 4.46; N, 11.63%.

Synthesis of $[(Cu(PPh_3)_2)_2(tdat)][BF_4]_2$, (4). Under nitrogen, a solution of tdat (0.025 g, 0.043 mmol) in CH_2Cl_2 was layered with $[Cu(CH_3CN)_2(PPh_3)_2][BF_4]$ (0.097 g, 0.14 mmol) dissolved in the same solvent. The molar ratio of the two compounds is 1 : 3. A subsequent layer of hexanes was then added. The solutions were allowed to slowly diffuse over several days. Colorless crystals of **4** were isolated in 41% yield. ^1H NMR (CD_2Cl_2, 500 MHz, 298 K, δ, ppm): 8.21 (br, 6H, py), 7.62 (br, 6H, py), 7.38 (t, $J = 8.0$ Hz, 12 H, ph), 7.22 (t, $J = 8.0$ Hz, 24 H, ph), 7.10 (broad and overlapping peaks, 24 H, Ph; 12 H, py). Mp 240 °C. Anal. calcd. for $C_{105}H_{84}N_{12}Cu_2P_4B_2F_8{\cdot}0.5CH_2Cl_2$: C, 63.92; H, 4.29; N, 8.48. Found: C, 63.89; H, 4.52; N, 8.04%.

Synthesis of $(AgNO_3)_{1.5}$(tab), (5). To a solution of tab (0.025 g, 0.059 mmol) in CH_2Cl_2, $AgNO_3$ (0.040 g, 0.234 mmol) dissolved in methanol (5 mL) was slowly added. $AgNO_3$ and tab were in a molar ratio of 1 : 4. The vial was covered with aluminum foil to prevent light-induced decomposition of the silver salt. The solvents were allowed to diffuse slowly over several days. The room temperature reaction produced brown transparent crystals of **5** in 82% yield. Mp 240 °C. ^1H NMR (DMSO-d_6, 300 MHz, 298K, δ, ppm): 8.46 (dd, $J = 4.8$ Hz, $J = 1.2$ Hz, 6H, 7-aza), 8.32 (s, 3H, benzene), 8.25 (dd, $J = 8.0$ Hz, $J = 1.2$ Hz, 6H, 7-aza), 8.19 (d, $J = 3.6$ Hz, 6H, 7-aza), 7.35 (dd, $J = 8.0$ Hz, $J = 4.8$ Hz, 6H, 7-aza), 6.87 (d, $J = 3.6$ Hz, 6H, 7-aza). ^{13}C NMR (DMSO-d_6, 300 MHz, 298K, δ, ppm): 146.5, 144.9, 138.7, 131.4, 130.1, 123.3, 118.3, 116.8. Anal. calcd. for $C_{27}H_{18}N_{7.5}O_{4.5}Ag_{1.5}{\cdot}H_2O$: C, 46.33; H, 2.86; N, 15.01. Found: C, 45.73; H, 2.34; N, 14.50%.

Synthesis of $(AgNO_3)_2$(tat), (6). On top of a solution of tat (0.025 g, 0.058 mmol) in CH_2Cl_2 (10 mL), $AgNO_3$ (0.040 g, 0.234 mmol) dissolved in excess methanol was layered. The molar ratio of the two components is 1 : 4. As in the reaction for **5**, the vial was covered with aluminum foil to prevent light-induced decomposition of the silver salt. After two days, the reaction at room temperature yielded crystals of compound **6** in 43% yield. Mp >300 °C (decomposition). ^1H NMR (methanol-d_4, 300 MHz, 298K, δ, ppm): 8.62 (dd, $J = 6.0$ Hz, $J = 2.1$ Hz, 2H, 7-aza), 8.51 (d, $J = 4.2$ Hz, 2H, 7-aza), 8.35 (d, $J = 5.1$ Hz, 4H, 7-aza), 8.26 (d, $J = 6.0$ Hz, 2H, 7-aza), 8.22 (d, $J = 8.1$ Hz, 4H, 7-aza), 7.51 (d, $J = 3.9$ Hz, 4H, 7-aza), 7.48 (d, $J = 5.4$ Hz, 2H, 7-aza), 7.26 (dd, $J = 8.0$ Hz, $J = 5.1$ Hz, 4H, 7-aza), 6.91 (d, $J = 4.2$ Hz, 2H, 7-aza), 6.64 (d, $J = 3.6$ Hz, 4H, 7-aza). Anal. calcd. for $C_{24}H_{15}N_{11}O_6Ag_2$: C, 37.47; H, 1.97; N, 20.03. Found: C, 37.21; H, 1.91; N, 19.35%.

Synthesis of $(AgNO_3)_4$(tdab), (7). A solution of tdab (0.051 g, 0.087 mmol) in CH_2Cl_2 (6 mL) was prepared and it was layered with benzene (4 mL), methanol (4 mL) and a sonicated solution of $AgNO_3$ (0.043 g, 0.251 mmol) in methanol (6 mL). The vial was covered with aluminum foil. The solvents were allowed to diffuse slowly yielding a yellow crystal in 35% yield. ^1H NMR (DMSO-d_6, 300 MHz, 298K, δ, ppm): 8.25 (d, $J = 4.5$ Hz, 6H), 7.70 (dd, $J \approx 7.7$ Hz, 6H), 7.05 (m, 12H), 6.50 (s, 3H). Anal. calcd. for

$C_{37}H_{31}N_{13}O_{12}Ag_4$: C, 34.26; H, 2.41; N, 14.04. Found: C, 33.93; H, 2.24; N, 13.88%.

Synthesis of $(AgNO_3)_3$(tdat), (8). Upon a solution of tdat (0.050 g, 0.0849 mmol) in CH_2Cl_2, benzene (4 mL), methanol (4 mL) and a sonicated solution of $AgNO_3$ (43 mg, 0.255 mmol) in methanol (6 mL) were successively layered. The vial was covered in aluminum foil and the solvents were allowed to diffuse slowly over several days, affording a white cotton ball-like powder of **8**. ^{1}H NMR (DMSO-d_6, 298K, 300 MHz, δ, ppm): 8.27 (d, J = 5.0 Hz, 6H), 7.76 (dd, J = 8.0 Hz, 6H), 7.47 (d, J = 8.0 Hz, 6H), 7.21 (dd, J = 5.0 Hz, J = 8.0 Hz, 6H). Anal. calcd. for $C_{33}H_{24}N_{15}O_9Ag_3{\cdot}2H_2O$: C, 34.85; H, 2.39; N, 18.47. Found: C, 34.84; H, 2.20; N, 18.43%.

Fluorescent titrations

All fluorescence titrations were performed at ambient temperature. Batch solutions of ligands tab and tdab (1×10^{-5} M in acetonitrile), tat and tdat (1×10^{-5} M in 4 : 1 acetonitrile–CH_2Cl_2) were prepared. The metal salts ($AgNO_3$ and $[Cu(CH_3CN)_2(PPh_3)_2][BF_4]$) were prepared in the same solvents used for the ligands. Prior to the addition of the metal salt solution to the ligand solution, the emission and excitation spectra for the free ligand solution were measured. Titrations were performed at one minute intervals to ensure that the solutions were at equilibrium. The emission spectra were recorded after each addition. For the titrations with $AgNO_3$, the vial was kept covered with aluminum foil to prevent any photo-induced decomposition.

X-Ray crystallographic analysis

Single crystals of complexes **1–7** were mounted on glass fibers for data collection. Data for **1**, **2** and **4–6** were collected on a Bruker Smart 1000 CCD X-ray diffractometer while data for **3** and **7** were collected on a Bruker Apex II single crystal X-ray diffractometer with graphite-monochromated Mo Kα radiation, operating at 50 kV and 30 mA, at either 298 K or 180 K. No significant decay was observed for any of the crystals. Data were processed on a PC using Bruker Apex II software and corrected for absorption effects. The structural solution and refinements were performed using the Bruker SHELXTL software package (version 6.14).[11a] All structures were solved by direct methods. Crystals **3**, **4**, and **6** belong to the triclinic space group P-1 while **1**, **2**, **5** and **7** belong to the monoclinic space groups $P2_1/n$, $P2_1/c$, $C2/c$, and Cc, respectively. Crystals **2** and **4** contain disordered CH_2Cl_2 solvent molecules (one per molecule of **2** and four per molecule of **4**) while crystals of **3** contain a disordered THF solvent molecule (one per molecule). To improve the quality of the structural data, the solvent molecules and their contributions were removed for these three molecules using the SQUEEZE routine in the PLATON program.[11b] The crystal data for **2–4** in Table 1 excluded contributions from solvent molecules in the lattice. The BF_4^- anions in the Cu(I) complexes **1–4** all display some degrees of disordering which were modeled and refined successfully. Some of the NO_3^- anions in the crystals of **5–7** are disordered which contributed to the poor quality of the structural data for **5** and **6** and as a consequence, the bond distances and angles for **5** and **6** are not as accurate as other molecules reported here. The crystals of **5** and **7** contain one CH_3OH solvent molecule per asymmetric unit, which was refined successfully. For **7**, there is a

Table 1 Crystal data for complexes **1–7**

	1	**2**	**3**	**4**	**5**	**6**	**7**
Formula	$C_{42}H_{30}BCuF_4N_9P$	$C_{45}H_{33}BCuF_4N_6P{\cdot}CH_2Cl_2$	$C_{54}H_{42}BCuF_4N_9P{\cdot}C_4H_8O$	$C_{105}H_{84}B_2Cu_2F_8N_1P_4{\cdot}4CH_2Cl_2$	$C_{54}H_{36}Ag_3N_{15}O_9{\cdot}2CH_3OH$	$C_{48}H_{30}Ag_4N_{22}O_{12}$	$C_{37}H_{31}Ag_4N_{13}O_{13}$
Fw	842.07	924.02	1070.39	2273.09	1426.67	1538.42	1297.23
Space group	$P2_1/n$	$P2_1/c$	P-1	P-1	$C2/c$	P-1	Cc
a/Å	15.009(4)	12.115(4)	11.2570(1)	14.823(4)	29.138(11)	10.365(5)	15.0865(3)
b/Å	14.840(4)	14.578(4)	15.4097(2)	17.746(5)	9.961(4)	10.661(5)	17.9907(4)
c/Å	17.565(5)	23.231(7)	15.5266(2)	21.116(5)	19.959(8)	12.142(6)	15.2317(3)
α/°	90	90	81.520(1)	83.863(5)	90	100.933(8)	90
β/°	98.363(6)	92.189(5)	85.3200(1)	81.498(6)	112.053(7)	94.262(8)	90.281(1)
γ/°	90	90	69.1880(1)	77.153(5)	90	115.538(7)	90
V/Å^3	3870.8(19)	4100(2)	2488.85(5)	5340(2)	5369(3)	1170.0(9)	4134.09(15)
Z	4	4	2	2	4	1	4
D_{calc}/g cm^{-3}	1.445	1.497	1.428	1.414	1.765	2.183	2.092
μ/cm^{-1}	6.70	7.64	5.39	7.26	11.62	17.46	20.84
T/K	293(2)	180(2)	180(2)	296(2)	180(2)	180(2)	296(2)
$2\theta_{max}$/°	52.00	52.00	54.30	50.00	52.00	52.00	52.00
No. of reflns measd	20499	19058	23805	24845	13863	7037	8043
No. of reflns used (R_{int})	7602 (0.0273)	8002 (0.0476)	10992 (0.0183)	16884 (0.0277)	5260 (0.1073)	4514 (0.0942)	5738 (0.0201)
No. of params	532	553	667	1215	389	388	607
R [$I > 4\sigma(I)$]:	0.0443	0.0528	0.0391	0.0560	0.0806	0.0729	0.0492
$R_1{}^a$ w$R_2{}^b$	0.0931	0.1143	0.1120	0.1413	0.1794	0.1180	0.1184
R (all data) $R_1{}^a$	0.0770	0.0863	0.0471	0.0881	0.2034	0.1821	0.0525
w$R_2{}^b$	0.1109	0.1237	0.1162	0.1544	0.2342	0.1375	0.1219
GOF on F^2	1.060	1.029	1.079	0.957	1.020	0.847	1.034

^{a} $R1 = \Sigma[|F_o| - |F_c|]/\Sigma|F_o|$. ^{b} $wR2 = \{\Sigma[w(F_o^2 - F_c^2)]/\Sigma(wF_o^2)\}^{1/2}$. $\omega = 1/[\sigma^2(F_o^2) + (0.075P)^2]$, where $P = [\max.(F_o^2, 0) + 2F_c^2]/3$.

large residual electron density (3.99 e Å^{-3}) which is at 1.01 Å away from Ag(1), attributable to the partial twinning of the crystal. All non-hydrogen atoms were refined anisotropically. The positions of hydrogen atoms were calculated, and their contributions in structural factor calculations were included. The crystal data for all complexes are summarized in Table 1. Important bond lengths and angles for all the compounds are listed in Table 2.

Results and discussions

Syntheses

The ligands tat, tab, tdab and tdat were obtained using procedures reported previously by our group.[5] The copper(I) complexes **1–4** were obtained by the reactions of the appropriate ligands with the common starting material $[Cu(CH_3CN)_2(PPh_3)_2][BF_4]$ while the Ag(I) complexes **5–8** were obtained by the reactions of the appropriate ligands with $AgNO_3$.

Complexes **1–3** are mononuclear Cu(I) complexes with the formula of $[Cu(PPh_3)(tat)][BF_4]$, $[Cu(PPh_3)(tab)][BF_4]$ and $[Cu(PPh_3)(tdab)][BF_4]$, respectively. The fact that all three compounds were isolated in good yields from the reaction of the chelate ligand with two or more equivalents of Cu(I) ions, seems to indicate that these mononuclear Cu(I) complexes may be thermodynamically favored products. The common feature among the three compounds is that there is only one PPh_3 ligand in the complex, which is quite surprising since Cu(I) ions are well known to have a high affinity toward phosphine ligands. The ^{1}H NMR spectra of these three complexes display broad peaks at ambient temperature and complex patterns at low temperature that are consistent with the presence of dynamic exchange in solution. Complex **4** is a dinuclear Cu(I) complex with the formula of $\{[Cu(PPh_3)_2]_2(tdat)\}[BF_4]_2$ where each Cu(I) center is associated with two PPh_3 ligands. Trinuclear Cu(I) complexes were not isolated from any of the ligand systems, despite the use of a large excess of Cu(I) starting material. Although complexes **1–4** were isolated as the major products from the tat, tab, tdab and tdat ligand systems, it is very likely that these are not the only products from the reactions. The complex dynamic behavior of the Cu(I) complexes in solution made it impossible to identify and characterize the minor products formed in the reactions. Therefore our investigation focuses on the major products that we can isolate and fully characterize.

The Ag(I) complexes **5–7** $(AgNO_3)_{1.5}(tab)$, $(AgNO_3)_2(tat)$, and $(AgNO_3)_4(tdab)$, were obtained from the reactions of the corresponding ligands with excess $AgNO_3$ (typically 3 or 4 equivalents), in good or modest yields. Ligand tdat forms cotton-ball-like solids with $AgNO_3$ that were found to have the formula of $(AgNO_3)_3(tdat)(H_2O)_2$ (**8**). Attempts were made to vary the stoichiometry of Ag(I) *versus* the ligand to isolate complexes that have different stoichiometry from those of **5–8**. However, regardless of the ratio of $AgNO_3$: ligand used in the actual reaction, complexes **5–8** were isolated consistently as the major products. All Ag(I) complexes are insoluble in common organic solvents such as methanol, CH_2Cl_2, and THF. The only solvent in which they are soluble in is DMSO. As a result, the ^{1}H NMR spectra of all Ag(I) complexes were recorded in DMSO. To establish the metal–ligand interactions and the bonding modes of the tat, tab, tdat and tdab ligands with Cu(I) and Ag(I) ions, single

Table 2 Selected bond lengths (Å) and angles (°)

Compound **1**			
Cu(1)–P(1)	2.2106(10)	P(1)–Cu(1)–N(2)	127.64(7)
Cu(1)–N(2)	2.008(2)	P(1)–Cu(1)–N(4)	107.85(8)
Cu(1)–N(4)	2.050(2)	P(1)–Cu(1)–N(7)	111.04(7)
Cu(1)–N(7)	2.132(2)	N(2)–Cu(1)–N(7)	88.48(10)
		N(2)–Cu(1)–N(4)	121.25(10)
		N(4)–Cu(1)–N(7)	88.49(10)
Compound **2**			
Cu(1)–P(1)	2.2279(11)	P(1)–Cu(1)–N(5)	135.36(9)
Cu(1)–N(4)	2.076(3)	P(1)–Cu(1)–N(4)	102.50(8)
Cu(1)–N(5)	2.018(3)	N(4)–Cu(1)–N(5)	115.82(11)
Cu(1)···C(26)	2.429(3)		
Compound **3**			
Cu(1)–P(1)	2.2027(5)	P(1)–Cu(1)–N(2)	122.17(5)
Cu(1)–N(1)	2.0779(15)	P(1)–Cu(1)–N(1)	121.87(5)
Cu(1)–N(2)	2.0609(17)	N(1)–Cu(1)–N(2)	107.69(6)
Cu(1)···C(35)	2.3110(18)		
Compound **4**			
Cu(1)–P(1)	2.2721(12)	P(1)–Cu(1)–N(10)	110.20(9)
Cu(1)–P(2)	2.2667(13)	P(1)–Cu(1)–N(12)	107.12(9)
Cu(1)–N(10)	2.169(3)	P(1)–Cu(1)–P(2)	120.27(4)
Cu(1)–N(12)	2.113(3)	P(2)–Cu(1)–N(10)	98.53(9)
Cu(2)–P(3)	2.2507(11)	P(2)–Cu(1)–N(12)	125.23(9)
Cu(2)–P(4)	2.2736(12)	P(3)–Cu(2)–N(1)	119.65(9)
Cu(2)–N(1)	2.102(3)	P(3)–Cu(2)–N(2)	113.56(9)
Cu(2)–N(2)	2.084(3)	P(3)–Cu(2)–P(4)	116.71(5)
		P(4)–Cu(2)–N(1)	106.36(9)
		P(4)–Cu(2)–N(2)	107.30(10)
		N(10)–Cu(1)–N(12)	88.72(12)
Compound **5**			
Ag(1)–N(2)	2.201(11)	N(2)–Ag(1)–N(2A)	160.8(6)
Ag(1)–O(4)	2.43(2)	N(2A)–Ag(1)–O(4)	82.9(7)
Ag(2)–N(6)	2.260(9)	N(2)–Ag(1)–O(4)	116.2(7)
Ag(2)–N(4)	2.360(10)	N(6)–Ag(2)–N(4)	118.5(3)
Ag(2)–O(1)	2.417(9)	N(6)–Ag(2)–O(1)	145.9(3)
Ag(2)–O(1A)	2.611(10)	N(4)–Ag(2)–O(1)	95.5(3)
Ag(2)···C(25)	2.685(13)	Ag(2)–O(1)–Ag(2A)	107.1(3)
Compound **6**			
Ag(1)–O(5)	2.520(9)	N(1)–Ag(1)–N(5)	75.5(3)
Ag(1)–N(1)	2.589(10)	N(1)–Ag(1)–O(2A)	117.8(3)
Ag(1)–N(5)	2.204(9)	N(1)–Ag(1)–O(5)	112.5(3)
Ag(1)–O(2A)	2.282(9)	N(5)–Ag(1)–O(2A)	130.5(3)
Ag(2)–O(2)	2.318(8)	N(5)–Ag(1)–O(5)	118.2(3)
Ag(2)–N(2)	2.617(9)	N(2)–Ag(2)–N(7)	71.8(3)
Ag(2)–N(7)	2.271(9)	N(2)–Ag(2)–N(9)	71.1(3)
Ag(2)–N(9)	2.327(10)	N(2)–Ag(2)–O(2)	108.4(3)
Ag(2)–O(4A)	2.511(10)	N(2)–Ag(2)–O(4)	157.3(3)
		N(7)–Ag(2)–N(9)	101.8(3)
		N(7)–Ag(2)–O(4A)	123.2(3)
		N(9)–Ag(2)–O(2)	117.1(3)
		N(9)–Ag(2)–O(4A)	88.2(4)
Compound **7**			
Ag(1)–N(1)	2.288(8)	N(1)–Ag(1)–N(4)	173.3(3)
Ag(1)–N(4)	2.288(8)	N(1)–Ag(1)–C(34)	86.2(3)
Ag(1)···C(34)	2.649(11)	N(4)–Ag(1)–C(34)	87.1(3)
Ag(2)–N(2)	2.316(8)	N(2)–Ag(2)–N(8)	167.4(3)
Ag(2)–N(8)	2.343(8)	N(2)–Ag(2)–C(36)	86.6(3)
Ag(2)···C(36)	2.635(11)	N(8)–Ag(2)–C(36)	85.5(3)
Ag(3)–N(5)	2.254(9)	N(5)–Ag(3)–O(2)	142.1(3)
Ag(3)–O(2)	2.447(10)	N(5)–Ag(3)–O(4)	104.5(4)
Ag(3)–O(4)	2.451(11)	O(2)–Ag(3)–O(4)	111.9(4)
Ag(4)–N(9)	2.237(9)	N(9)–Ag(4)–O(7)	140.0(3)
Ag(4)–O(7)	2.448(10)	N(9)–Ag(4)–O(8)	158.1(3)
Ag(4)–O(8)	2.540(11)	O(7)–Ag(4)–O(8)	51.5(3)
Ag(1)···O(7A)	2.654(10)		
Ag(1)···O(9A)	2.655(10)		
Ag(2) ··· O(2A)	2.706(11)		
Ag(2)···O(3A)	2.761(10)		
Ag(2)···O(11)	2.666(10)		
Ag(3)···O(1)	2.603(10)		
Ag(4)···O(1A)	2.715(10)		
Ag(4)···O(11)	2.752(10)		

crystal X-ray diffraction analyses were conducted for complexes **1–7**. For complex **8**, repeated attempts failed to produce adequate single crystals for X-ray study. Nonetheless, the cotton-ball-like appearance of the crystals of **8** is an indication that **8** likely has a polymeric structure in the solid state.

Crystal structures of 1–7

[Cu(PPh$_3$)(tat)][BF$_4$], (1). As shown in Fig. 1, the Cu(1) atom in **1** is coordinated by two 7-azaindolyl groups and one PPh$_3$. In addition, the Cu(1) is bound to N(7) in the triazine ring with a normal bond length of 2.132(2) Å, which is somewhat longer than those of Cu(1)–N (7-azaindolyl) bonds. As a result, the geometry around the Cu(1) center may be described as a distorted tetrahedron. Notably, despite the coordination by a Cu(I) ion, the tat ligand adopts a nearly planar conformation, as evidenced by the small dihedral angles between the central triazine ring and the three 7-azaindolyl rings (3.2°, 8.0° and 23.2° for the N(6), N(4) and N(2) ring, respectively). This can be attributed to the enhanced π-conjugation between the 7-azaindolyl and the N atoms of the triazine ring; another contributor is the favorable H-bond interactions between the C$_2$-H of the 7-azaindolyl and the N atoms from the triazine. The average C–N distance between the 7-azaindolyl and the triazine (1.385(4) Å) further suggests the presence of strong π-conjugations. In addition, intramolecular π–π stacking exists between the pyrrole ring of the 7-azaindolyl and one phenyl ring of PPh$_3$ as evidenced by the short atomic separation distances between them (~3.6 Å on average). This conformation may prevent exchange processes from occurring, and, more specifically, may prevent the Cu(I) from migrating to the other uncoordinated sites.

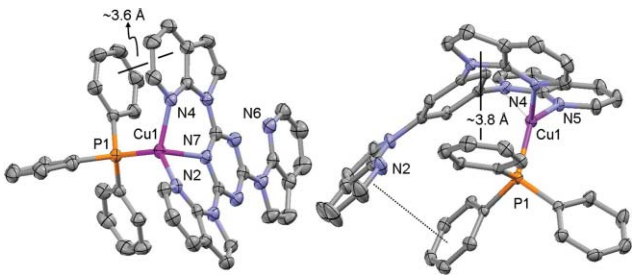

Fig. 1 Diagrams showing the structure of **1** (left) and **2** (right) with 30% thermal ellipsoids.

[Cu(PPh$_3$)(tab)][BF$_4$], (2). The structure of **2** has some resemblance to that of **1**, as shown in Fig. 1. The Cu(1) center is chelated by two 7-azaindolyl groups and one PPh$_3$ group. Although there is a short contact distance between Cu(1) and C(26) in the central benzene ring in **2** (2.429(3) Å), the Cu(1) atom is clearly 3-coordinate with a somewhat distorted trigonal planar geometry. The coordination environment of the Cu(I) center in **2** resembles that of {[Cu(PPh$_3$)]$_2$(ttab)}[BF$_4$]$_2$ (ttab = 1,2,4,5-tetrakis(*N*-7-azaindolyl)benzene).[12] Despite the use of excess Cu(I) starting material in the reaction, as observed for **1**, the 3rd 7-azaindolyl group remains uncoordinated. In contrast to the structure of **1** where the entire tat ligand is coplanar, the three 7-azaindolyl rings in **2** are not coplanar with the central benzene ring, but have a fairly large dihedral angle (29.4, 45.1 and 48.4°, for the N(2), N(4) and N(5) rings, respectively.). The C–N bonds between the 7-azaindolyl and the central benzene ring are also notably longer than those in **1** (1.421(4) Å). This suggests the presence of reduced π conjugation between the 7-azaindolyl and the benzene ring. Factors include both steric repulsion between the C$_2$-H of 7-azaindolyl and the H atoms in the central phenyl ring and the reduced electronegativity of the carbon atoms compared to the nitrogen atoms in the benzene and triazine cores respectively. The tab ligand appears to wrap around the Cu(I) center, encasing it, a consequence of the lack of planarity. As in **1**, intramolecular π–π stacking is evident between the pyrrole ring of a 7-azaindolyl and a phenyl ring of PPh$_3$. However, additional intramolecular π–π stacking exists between the non-coordinate 7-azaindolyl ring and another phenyl group (the shortest separation distance is ~3.55 Å). In principle it is possible for the [Cu(PPh$_3$)]$^+$ group to migrate between different 7-azaindolyl groups, although the π–π interactions between the aromatic rings may prevent it from doing so.

[Cu(PPh$_3$)(tdab)][BF$_4$], (3). The tdab ligand contains 6 pyridyl groups which can potentially chelate to three Cu(I) ions. Our earlier investigation of Zn(II) and Pt(II) complexes with tdab showed that chelation always involved the two pyridyl rings bound to the same nitrogen atom.[6] In comparison with the earlier findings, the structure of **3** shown in Fig. 2 is rather surprising and interesting. First of all, as observed in complexes **1** and **2**, the Cu(I) ion is only bound by one PPh$_3$ ligand. In addition, it is coordinated by two pyridyl groups that are not bound to the same nitrogen atom with a trigonal planar geometry, similar to that in **2**. The separation distance between a carbon atom (C(35)) in the central benzene ring and the Cu(1) atom (2.311(1) Å) is much shorter than that observed in **2**. Although various intramolecular interactions between the phenyl groups of PPh$_3$ and the pyridyls are present, they are not as well defined as those in **1** and **2**. Some of the intramolecular interactions appear to be edge-on, not stacking. One interesting feature is that the phosphorus atom is situated directly above the centre of the benzene core ring (separation distance of 3.853(1) Å). As observed in **2**, the tdab ligand wraps around the Cu(I) center in **3**, which appears to provide good protection of the Cu(I) center. Nonetheless, there are four non-coordinating pyridyl groups in **3** that may compete for the Cu(I) center in solution.

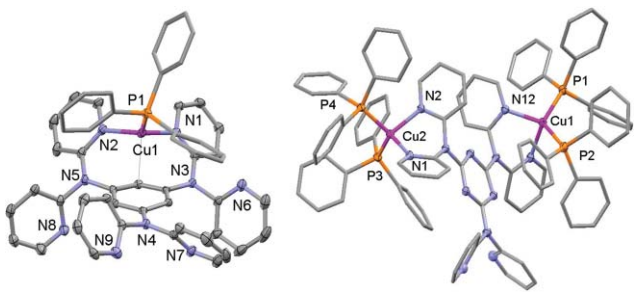

Fig. 2 Diagrams showing the structure of **3** (left) and **4** (right) with 30% thermal ellipsoids. For clarity, all carbon atoms in **4** are shown in capped stick styles.

[(Cu(PPh$_3$)$_2$)$_2$ (tdat)][BF$_4$]$_2$, (4). The tdat ligand is an analogue of tdab except that the central core is a triazine ring, instead of a benzene ring. The structure of **4** shown in Fig. 2 is in sharp contrast to those of **1–3**. Instead of one PPh$_3$ with each Cu(I)

ion as observed in **1–3**, both Cu(I) ions in **4** are bound by two PPh_3 groups. Furthermore, instead of the 'atypical' chelating mode shown by **3**, the Cu(I) ion in **4** is bound to two pyridyl groups with a 'normal" chelate mode, with both pyridyl groups from the same dipyridylamino unit. As a result, the Cu(I) centers in **4** display distorted tetrahedral geometry. With respect to the triazine ring, the two $[Cu(PPh_3)_2]^+$ units appear on opposite sides, perhaps to avoid steric interactions. The distance between Cu(1) and Cu(2) is 8.94(1) Å. The structure of **4** confirms that the "normal" dipyridylamino chelate mode of tdat or tdab to a $[Cu(PPh_3)_2]^+$ unit is possible. Therefore, the unusual bonding mode displayed by tdab and the loss of one phosphine ligand in **3** cannot be attributed to simple steric or electronic effects of the ligand since the chelate groups in tdab and tdat are identical. In **4**, one of the dipyridylamino groups does not coordinate. As a result, dynamic exchange of **4** in solution is possible.

$(AgNO_3)_{1.5}$(tab), (5). As shown in Fig. 3, in the asymmetric unit of the crystal of **5**, there are two types of Ag(I) environment: one being chelated by two 7-azaindolyl groups of the tab ligand (Ag(2)) and one being bound by a single 7-azaindolyl group (Ag(1)). The Ag(2) atom has a short contact distance of 2.685(13) Å with C(25) in the central benzene ring. In addition, one nitrate anion is bound to the Ag(2) center *via* one oxygen atom, resulting in an approximate trigonal planar geometry around the Ag(2) center. The Ag(1) atom sits on a C_2 axis and is further bound by one 7-azaindolyl group from the C_2 symmetry related asymmetric unit in a near linear fashion (N(2)–Ag(1)–N(2A) = 160.8(6)°). As a result, two tab ligands link three Ag(I) ions together in **5** to form a helical structure as shown in Fig. 3. The three 7-azaindolyls are not coplanar with the central benzene ring as is evident in the large dihedral angles (58.0, 46.2 and 48.8° for N(1), N(3) and N(5) rings respectively). The binding modes of tab and the helical structure of **5** resemble that observed in $Pd_3(tab)_2Cl_4$ except that the C–H bond that is in close contact with Ag(2) in **5** is broken and becomes part of a N,C,N-chelate with the Pd center in the Pd_3 complex.[7] The Ag(1) ion is also bound by a disordered nitrate anion with a long Ag(1)–O(4) bond (2.43(2) Å). Two CH_3OH solvent molecules are bound to the latter nitrate *via* hydrogen bonds. This Ag_3 unit is further linked together by a NO_3^- *via* the oxygen atom (O(1)) that acts as a bridging ligand for Ag(2) and Ag(2A) (Ag(2)-O(1)-Ag(2A) = 107.1(3)°), leading to the formation of a 1D chain shown in Fig. 3.

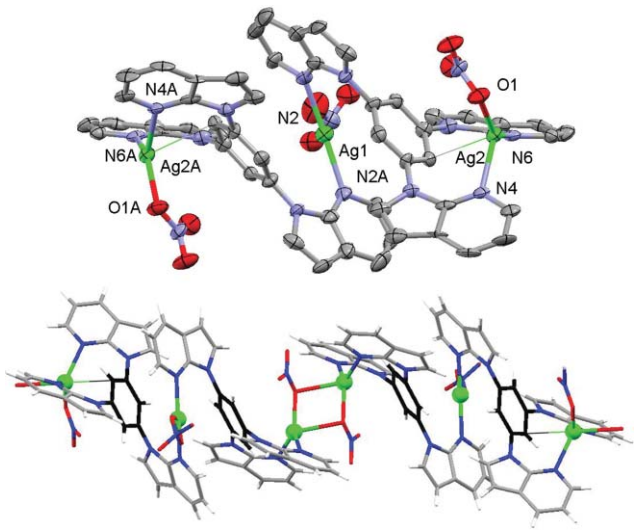

Fig. 3 Top: a diagram showing the $(AgNO_3)_3(tab)_2$ unit in **5** with 30% thermal ellipsoids. Bottom: A diagram showing the 1D structure of **5**, the central phenyl ring is shown in black color.

$(AgNO_3)_2$(tat), (6). In the asymmetric unit of **6**, there are two $AgNO_3$ groups attached to the tat ligand. Two of the 7-azaindolyl groups are chelated to Ag(2) while the 3rd one is bound to Ag(1) in a manner similar to that observed in **5**. Most significant are the short separation distances between the two Ag(I) ions and two of the nitrogen atoms in the triazine ring (Ag(1)–N(1) = 2.589(10) Å, Ag(2)–N(2) = 2.617(9) Å), suggesting some degree of binding interaction. Compared to those in **5**, the three 7-azaindolyls in **6** are more coplanar with the central triazine ring, as evidenced by the much smaller dihedral angles (23.9°, 30.2° and 19.5° for the N(4), N(6) and N(8) rings respectively), consistent with the trend observed for **1** and **2**. Perhaps as a consequence of the conformation difference of tab *versus* tat in **5** and **6**, these two molecules have distinct stoichiometry and extended structures. The NO_3^- bound to Ag(2) forms a bond with Ag(1A) from an inversion center-related neighboring asymmetric unit *via* an oxygen atom bridge, O(2), with Ag(1A)–O(2) = 2.282(9) Å and Ag(2)–O(2)–Ag(1A) = 135.3(4)°. The O(1) atom in the same nitrate group has a weak bond with Ag(1A), as evidenced by the Ag(1A)–O(1) distance of 2.709(10) Å. As a result, molecule **6** has an unusual sandwich structure with four Ag(I) ions being sandwiched between two tat ligands, as shown in Fig. 4. This sandwich structure is further extended by the nitrate on Ag(1) that forms a bond with Ag(2A) in the neighboring unit *via* the O(4) atom, (Ag(2)–O(4′) = 2.511(10) Å), resulting in an intriguing 1D sandwich chain, as shown in Fig. 4. There are extensive π–π stacking interactions between the 1D chains.

$(AgNO_3)_4$(tdab), (7). In the asymmetic unit of the crystal of **7**, there are four $AgNO_3$ groups attached to one tdab ligand. As shown in Fig. 5, the 6 pyridyl groups in tdab display two different bonding modes with the Ag(I) ions: chelating and terminal binding. Four pyridyl groups are chelated to Ag(1) and Ag(2), respectively, with a near linear geometry (N(1)–Ag(1)–N(4) = 173.3(3)°, N(2)-Ag(2)-N(8) = 167.4(3)°). Again, as observed in the structure of **3**, the two chelating pyridyl groups on Ag(1) or Ag(2) center are not bound to the same nitrogen atom. For Ag(I) ions, such an "atypical" chelate mode by the two pyridyl groups may be explained by the preference for a linear geometry by the Ag(I) ion. The remaining two pyridyl groups act as terminal ligands to the Ag(3) and Ag(4) ions, respectively. Both Ag(1) and Ag(2) have a short contact distance with a carbon atom in the central benzene ring (Ag(1)···C(34) = 2.649(11) Å, Ag(2)···C(36) = 2.635(11) Å). Ag(4) and Ag(3) are bound by one and two NO_3^- anions respectively, with Ag–O distances ranging from 2.447(1) Å to 2.540(10) Å. The 4th NO_3^- is bound weakly to both Ag(2) and Ag(4) *via* the O(11) atom (Ag(2) ···O(11) = 2.666(10) Å, Ag(4) ···O(11) = 2.752(10) Å). All three dipyridylamino units in the tdab ligand are approximately perpendicular to the central benzene ring. As a result, the molecule of **7** has a chair-like structure. Most significantly, the NO_3^- anions that are bound to Ag(3) and Ag(4) also form weak bonds with Ag(1) and Ag(2)

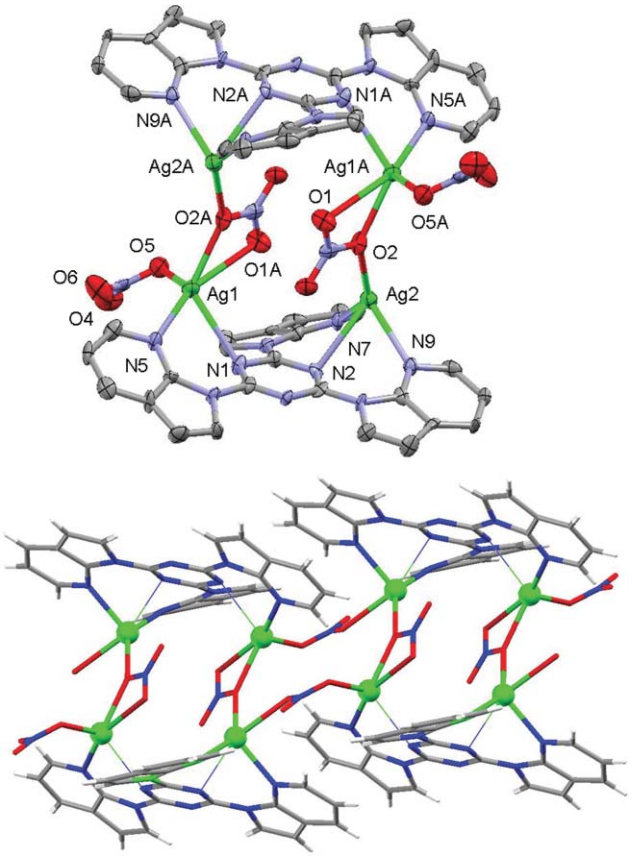

Fig. 4 Diagrams showing the $(AgNO_3)_4(tat)_2$ unit of **6** (top) with 30% thermal ellipsoids and the 1D structure (bottom).

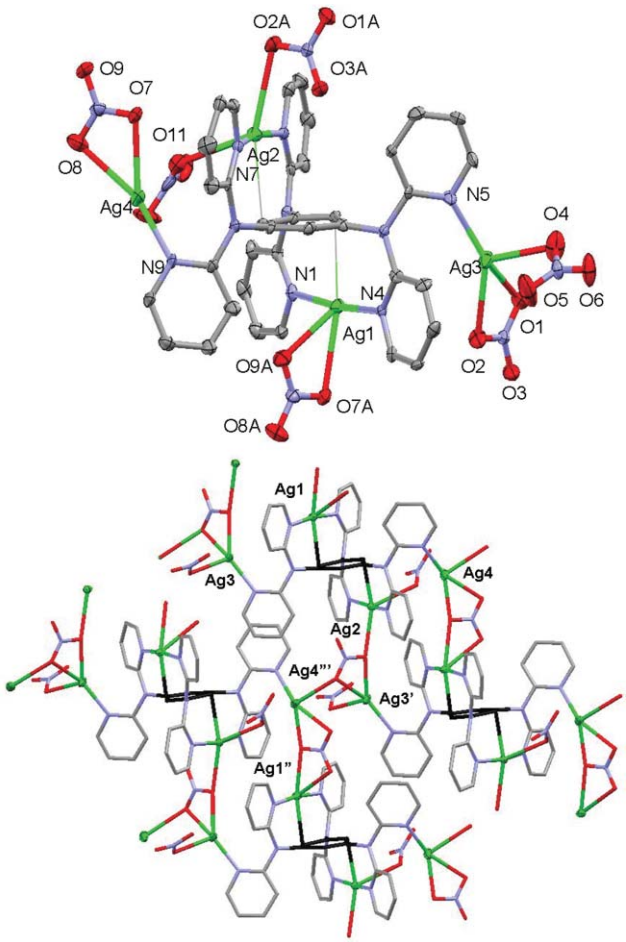

Fig. 5 Diagrams showing the $[(AgNO_3)_4(tdab)]$ unit of **7** along with nitrate anions from neighboring asymmetric units (O(1A) and O(7A)) (top) and the 2D structure involving 4 Ag_4 units (bottom) with the central benzene rings shown in black color.

atoms in the neighboring asymmetric units (see Table 2). Ag(3) and Ag(4) from two neighboring units are also linked together by a nitrate anion as shown in Fig. 6. As a result of the extensive binding interactions between the Ag(I) ions and the nitrate, **7** forms a 2D extended network that stacks to form a 3D layered crystal lattice, as shown in Fig. 6. A methanol solvent molecule was located in the asymmetric unit that is hydrogen-bonded to a nitrate oxygen atom (O(10)).

Compared to the corresponding Cu(I) complexes, there are two distinct features displayed by the Ag(I) complexes. First, all binding sites on the chelate ligands are occupied by the Ag(I) ions in **5–7**, whereas in the copper complexes, only some of the binding sites are occupied by metal ions. Second, all Ag(I) complexes are polymeric while all the copper complexes are discrete molecules. These differences can in part be attributed to the presence of the phosphine ligand in the copper complexes that saturates the coordination sphere of Cu(I), thus preventing the formation of polymeric species. Furthermore, the steric bulk of the PPh_3 ligand also limits the number of Cu(I) ions that can access the same chelate ligand. The highly flexible coordination sphere around the Ag(I) ion, compared to the relatively rigid geometry/coordination number around the Cu(I) center, also facilitates the formation of polymeric structures.

Dynamic exchange in solution by complexes 1–7

The presence of unoccupied binding sites in complexes **1–4** as established by the crystal structures makes it possible for the Cu(I) ion to undergo dynamic site exchange in solution. To determine if this is indeed the case, we examined the ^{1}H NMR spectra of complexes **1–4** at various temperatures. For complex **1**, due to the coplanarity of the tat ligand and the chelation to a Cu(I) ion, each 7-azaindolyl group has a distinct chemical environment in the solid state. Hence, if **1** retains the same structure in solution, three sets of peaks for the three 7-azaindolyl groups should be observed in the ^{1}H NMR spectrum. At ambient temperature, instead of three sets, we observed two sets of well resolved 7-azaindolyl peaks in a 2 : 1 ratio which can be assigned to coordinated and non-coordinated 7-azaindolyl rings. The non-coordinated 7-azaindolyl ring is likely to be rotating rapidly around the N–C (triazine) bond in solution, resulting in the exchange of the two coordinated 7-azaindolyl rings. As temperature decreases, a new set of 7-azaindolyl peaks appear as shown in Fig. 6, and the resulting NMR spectrum is consistent with the crystal structure of **1**. Thus, we can conclude that the dynamic exchange in **1** is caused by the rotation of the non-coordinated 7-azaindolyl group, not the migration of the Cu(I) ion. The behavior of **2** resembles that of **1**.

The behavior of complex **3** is quite different. At ambient temperature, as shown in Fig. 6, the ^{1}H NMR spectrum of **3** displays only one set of pyridyl peaks and one single peak for the three protons in the central benzene ring, consistent with the

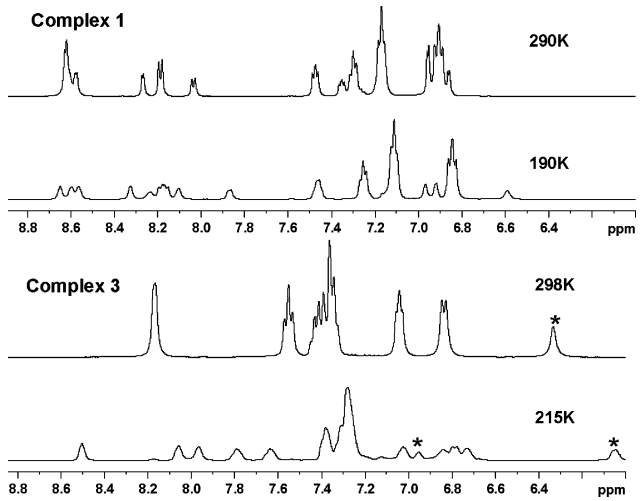

Fig. 6 ^{1}H NMR spectra of **1** (top) and **3** (bottom) recorded in CD_2Cl_2 at ambient temperature and low temperature, respectively. The peaks from the central benzene ring in **3** are marked by *. The full variable temperature NMR spectra can be found in the ESI† (Fig. S1–S4).

presence of dynamic exchange between the two coordinated and the four non-coordinated pyridyl rings. At low temperature, the ^{1}H NMR spectrum of **3** displays a complex pattern with multiple sets of pyridyl peaks that cannot be fully assigned due to extensive peak overlapping. Nonetheless, the three protons in the central benzene ring are resolved into two sets of peaks with a 2 : 1 ratio at 215 K (their assignments are based on COSY data), which is consistent with the crystal structure. Similarly, the ^{1}H NMR spectrum of complex **4** displays only one set of broad pyridyl peaks at ambient temperature, indicating that all pyridyl rings in **4** also undergo a dynamic exchange process in solution. Thus, in contrast to complexes **1** and **2**, the Cu(I) ion in **3** and **4** is most likely migrating between the different binding sites, causing the dynamic exchange of the pyridyl groups.

The distinct solution behavior of the tat and tab complexes *versus* the tdab and tdat complexes may be explained by the fact that in tat and tab, there are only three 7-azaindolyl groups that can bind to the Cu(I) center while in tdab and tdat there are six pyridyl groups available for Cu(I) binding. In addition, the non-coordinating 7-azaindolyl group is further away from the Cu(I) center in **1** and **2**, compared to the non-coordinate pyridyl groups in **3** and **4**, thus making it more difficult for the Cu(I) ions in **1** and **2** to migrate from one site to another than those in **3** and **4**. Similar dynamic exchanges have been previously observed in the mononuclear and dinuclear $ZnCl_2$ complexes[6a] of tdab and tdat and the complex[6b] of $(PdCl_2)$(tdab). Hence, the dynamic exchange observed for **3** and **4** can be attributed to the inherent propensity of the tdab and tdat ligands for pyridyl site exchange in coordination unsaturated complexes.

For the Ag(I) complexes **5** and **6**, the three 7-azaindolyl groups in the tab and tat ligands have two distinct environments: chelating and terminal. In solution, however, only one set of 7-azaindolyl peaks are observed in the ^{1}H NMR spectrum in DMSO at 298 K for both complexes. They are distinctively different from those of their respective free ligands, indicating that the Ag(I) ions are still bound to the tab or tat ligand with the three 7-azaindolyl groups undergoing rapid dynamic exchange. Due to the insolubility of the Ag(I) complexes in solvents other than DMSO, variable temperature NMR spectra could not be recorded. Although the crystal structure shows that there are clearly two different types of pyridyl groups in **7**, the ^{1}H NMR spectrum of **7** recorded in DMSO shows only one set of pyridyl peaks that resembles that of the free ligand, tdab, an indication of dynamic exchange among the pyridyl groups and the dissociation of the Ag(I) ions from the ligand in solution. The dynamic exchange of the Ag(I) complexes is most likely facilitated by the coordinating DMSO solvent molecules that can compete for the Ag(I) center. Again, due to the poor solubility of **7** in solvents other than the coordinating DMSO solvent, a detailed NMR study on its dynamic behavior in solution could not be performed.

Fluorescent response of tat, tab, tdab and tdat ligands towad Cu(I) and Ag(I)

Ligands tat, tab, tdat and tdab are all fluorescent with the emission maxima ranging from 345 to 400 nm in solution. One convenient way to study the interactions of Cu(I) and Ag(I) with these ligands is to examine their fluorescent responses toward Cu(I) and Ag(I) ions. We therefore carried out fluorescence titration experiments of the four ligands with $[Cu(CH_3CN)_2(PPh_3)_2][BF_4]$ and $AgNO_3$. For each fluorescence titration experiment, we did the UV-Vis titration in parallel. The UV-Vis titration data can be found in the ESI† (S9 and S10), which support unequivocally that the fluorescent change with the addition of metal ions is not due to the change of absorbance because at the excitation wavelength (tat, 294 nm; tab, 298 nm; tdat, 295 nm; and tdab, 315 nm) used in the fluorescence titration experiments, there is either little change in absorbance or a slight increase in absorbance with the addition of metal ions.

Tat and tab. For the tat ligand, the addition of $[Cu(CH_3CN)_2(PPh_3)_2][BF_4]$ to its solution yields a dramatic fluorescent intensity increase that reaches a plateau after the addition of *ca.* one equivalent of Cu(I). Because the titration spectrum of tat with $[Cu(CH_3CN)_2(PPh_3)_2][BF_4]$ resembles that of $[Cu(PPh_3)(tat)][BF_4]$, (**1**), the fluorescent enhancement of tat can be attributed to the formation of complex **1**. The addition of $AgNO_3$ to the solution of tat initially results in a slight quenching of the emission peak and little change is observed after the addition of more than 2 equivalents of Ag(I) (see ESI† and Fig. 7). Due to the poor solubility of the Ag(I) complexes in solvents other than DMSO, the fluorescence spectra of complexes **5–7** were not recorded. Comparisons between the titration spectra and those of the complexes could not therefore be achieved for the Ag(I) ions. Despite the structural similarity of tab and tat, the response of tab toward Cu(I) and Ag(I) is quite different from that of tat. Instead of the intensity gain, the addition of $[Cu(CH_3CN)_2(PPh_3)_2][BF_4]$ to the solution of tab causes a steady quenching of the emission peak, a response similar to that of ttab.[12] The addition of $AgNO_3$ to the solution of tab also results in significant quenching of the emission, indicative of the presence of binding interactions between the metal ion and the tab ligand in solution. The distinct response of tab and tat toward Cu(I) ions, albeit not fully understood, suggests that the nature of the central core in the ligand does have a significant impact on the photophysical properties of Cu(I) complexes.

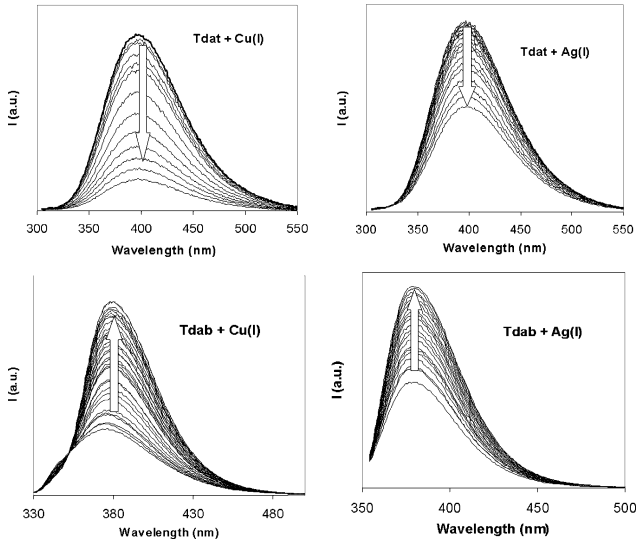

Fig. 7 Fluorescence titration diagrams of tdat (λ_{ex} = 295 nm) in 4 : 1 CH_3CN–CH_2Cl_2 and tdab (λ_{ex} = 315 nm) in CH_3CN with $[Cu(CH_3CN)_2(PPh_3)_2][BF_4]$ and $AgNO_3$, respectively. Titration diagrams of tat (λ_{ex} = 294 nm) and tab (λ_{ex} = 298 nm) can be found in the ESI†.

Tdat and tdab. For the tdat ligand, both $[Cu(CH_3CN)_2(PPh_3)_2][BF_4]$ and $AgNO_3$ cause significant and steady quenching of the tdat emission. However, for Ag(I) ions, a large excess is needed to cause significant quenching of tdat as shown by Fig. 7 and 8 Nonetheless, the fluorescent responses of Cu(I) and Ag(I) toward tdat are similar. Despite being a structural analogue of tdat, the response of tdab toward Cu(I) and Ag(I) is the opposite of tdat: instead of quenching, the metal ions cause fluorescent intensity increase. The addition of Cu(I) results in a fluorescence turn-on response as shown in Fig. 8, which reaches a plateau after the addition of *ca*. one equivalent of Cu(I). Again, the titration spectrum of tdab by Cu(I) is similar to the fluorescence spectrum of $[Cu(PPh_3)(tdab)][BF_4]$, (**3**), thus the drastic emission intensity increase can be attributed to the formation of complex **3**. The addition of $AgNO_3$ to the solution of tdab also causes a significant turn-on response that has a clear transition point at about three equivalents of Ag(I). As demonstrated by the crystal structures, both Cu(I) and Ag(I) ions chelate to the tdab ligand *via* two py ligands that are not bound to the same amino nitrogen. Perhaps it is this unique chelating mode that is responsible for the significant fluorescent enhancement of tdab upon binding with Cu(I) and Ag(I).

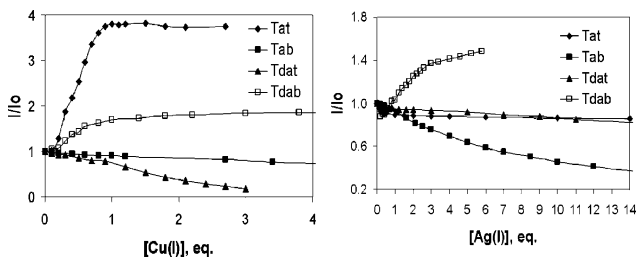

Fig. 8 The Stern–Volmer plots of fluorescence titrations by $[Cu(CH_3CN)_2(PPh_3)_2][BF_4]$ and $AgNO_3$.

The fluorescence titration experiments demonstrate that the central core of the ligands has a distinct impact on the luminescent responses of the 7-azaindolyl or 2′2-dipyridylamino, which may be attributed to the distinct structures of the complexes. However, the electronic properties of the central core and the conformation of the ligand may also be key factors. Nonetheless, because of the distinct response from the ligands with a triazine core *versus* that with a benzene core toward Cu(I) and Ag(I) ions, the combination of this group of ligands has the potential for use as fluorescent sensors for metal ions.

In summary, our investigation has established unequivocally that the tat, tab, tdat and tdab ligands form distinct structures with Cu(I) and Ag(I) ions that result in distinct fluorescent responses. The different central cores, benzene and triazine, in tat and tab, tdat and tdab, are clearly responsible for the observed structural and fluorescent differences.

Acknowledgements

We thank the Natural Sciences and Engineering Council of Canada for financial support of this work. We thank Dr. Rui-Yao Wang for his assistance in some of the crystal structural work.

References

1 (*a*) *Inorganic Materials*, ed. D. W. Bruce and D. O'Hare, 2nd edition, John Wliey & Sons, New York, 1996; (*b*) J. W. Steed, J. L. Atwood, *Supramolecular Chemistry*, John Wiley & Sons, New York, 2000; (*c*) *Extended Linear Chain Compounds*, ed. J. S. Miller, vol. I, Plenum, New York, 1982; (*d*) D. Tanaka and S. Kitagawa, *Chem. Mater.*, 2008, **20**, 922; (*e*) S. Kitagawa and R. Matsuda, *Coord. Chem. Rev.*, 2007, **251**, 2490; (*f*) B. D. Chandler, G. D. Enright, K. A. Udachin, S. Pawsey, J. A. Ripmeester, D. T. Cramb and G. K. H. Shimizu, *Nat. Mater.*, 2008, **7**, 229; (*g*) S. A. Dalrymple and G. K. H. Shimizu, *J. Am. Chem. Soc*, 2007, **129**, 12114; (*h*) M. J. Katz, H. Kaluarachchi, R. J. Batchelor, A. A. Bokov, Z.-G. Ye and D. B. Leznoff, *Angew. Chem., Int. Ed.*, 2007, 8804.

2 (*a*) Z. Shen, P. E. Burrows, V. Bulovic, S. R. Borrest and M. E. Thompson, *Science*, 1997, **276**, 2009; (*b*) M. A. Baldo, S. Lamansky, P. Burrows, M. E. Thompson and S. R. Forrest, *Appl. Phys. Lett.*, 1999, **75**, 5; (*c*) R. C. Kwong, S. Sibley, T. Dubovoy, M. Baldo, S. R. Forrest and M. E. Thompson, *Chem. Mater.*, 1999, **11**, 3709; (*d*) Q. D. Liu, L. Thorne, I. Kozin, D. Song, C. Seward, M. D'Iorio, Y. Tao and S. Wang, *J. Chem. Soc., Dalton Trans.*, 2002, 3234; (*e*) M. Buda, G. Kalyzuzhny and A. Bard, *J. Am. Chem. Soc.*, 2002, **124**, 6090; (*f*) B. O'Regan and M. Grätzel, *Nature*, 1991, **353**, 737.

3 (*a*) V. H. Houlding and V. M. Miskowski, *Coord. Chem. Rev.*, 1991, **111**, 145; (*b*) C. N. Pettijohn, E. B. Jochnowitz, B. Chuong, J. K. Nagle and A. Vogler, *Coord. Chem. Rev.*, 1998, **171**, 85; (*c*) H. Yersin, W. Humbs and J. Strasser, *Coord. Chem. Rev.*, 1997, **159**, 325; (*d*) W. Paw, S. D. Cummings, M. A. Mansour, W. B. Connick, D. K. Gieger and R. Eisenberg, *Coord. Chem. Rev.*, 1998, **171**, 125; (*e*) J. E. McGarrah, Y. J. Kim, M. Hissler and R. Eisenberg, *Inorg. Chem.*, 2001, **40**, 4510.

4 (*a*) Y. Sun, N. Ross, S. B. Zhao, K. Huszarik, W. L. Jia, R. Y. Wang, D. Macartney and S. Wang, *J. Am. Chem. Soc.*, 2007, **129**, 7510; (*b*) J. Lefebvre, R. J. Batchelor and D. B. Leznoff, *J. Am. Chem. Soc.*, 2004, **126**, 16117; (*c*) J. C. Vickery, M. M. Olmstead, E. Y. Fung and A. L. Balch, *Angew. Chem., Int. Ed. Engl.*, 1997, **36**, 1179; (*d*) J. Pang, E. J-,P. Marcotte, C. Seward, R. S. Brown and S. Wang, *Angew. Chem., Int. Ed.*, 2001, **40**, 4042.

5 J. Pang, Y. Tao, X.-P. Yang, M. D'Iorio and S. Wang, *J. Mater. Chem.*, 2002, **12**, 206.

6 (*a*) C. Seward, J. Pang and S. Wang, *Eur. J. Inorg. Chem.*, 2002, **6**, 1390; (*b*) C. Seward, W. L. Jia, R. Y. Wang and S. Wang, *Inorg. Chem.*, 2004, **43**, 978; (*c*) Q. D. Liu, W. L. Jia, G. Wu and S. Wang, *Organometallics*, 2003, **22**, 3781.

7 (*a*) D. T. Song, Q. Wu, A. Hook, I. Kozin and S. Wang, *Organometallics*, 2001, **20**, 4683; (*b*) Q. Wu, A. Hook and S. Wang, *Angew. Chem., Int. Ed.*, 2000, **39**, 3933.
8 (*a*) W. L. Jia, T. McCormick, Y. Tao, J. P. Lu and S. Wang, *Inorg. Chem.*, 2005, **44**, 5706; (*b*) Q. Zhang, Q. Zhou, Y. Cheng, L. Wang, D. Ma, X. Jing and F. Wang, *Adv. Mater.*, 2004, **16**, 432.
9 (*a*) C. Seward, W. L. Jia, R. Y. Wang, G. D. Enright and S. Wang, *Angew. Chem., Int. Ed. Engl.*, 2004, **43**, 2933; (*b*) C. Seward, J. Chan, D. Song and S. Wang, *Inorg. Chem.*, 2003, **42**, 1112.
10 (*a*) G. J. Kubas, B. Monzyk and A. L. Crumbliss, *Inorg. Synth.*, 1979, **19**, 90; (*b*) J. Diez, S. Falagan, P. Gamasa and J. Gimeno, *Polyhedron*, 1988, **7**, 37.
11 (*a*) *SHELXTL*, version 6.14, Bruker AXS, 2000; (*b*) A. L. Spek, *Acta Crystallogr., Sect. A*, 1990, **46**, C34; A. L. Spek, *PLATON A Multipurpose Crystallographic Tool*, Utrecht University, Utrecht, The Netherlands, 2006.
12 S. B. Zhao, R. Y. Wang and S. Wang, *Inorg. Chem.*, 2006, **45**, 5830.